

SIMULATION STUDY OF THE MAGNETIZED ELECTRON BEAM*

S.A.K. Wijethunga^{†1}, M.A. Mamun², F.E. Hannon², G.A. Krafft^{1,2}, J. Benesch²,
R. Suleiman², M. Poelker², J.R. Delayen¹

¹Old Dominion University, Norfolk, VA 23529, USA

²Thomas Jefferson National Accelerator Facility, Newport News, VA 23606, USA

Abstract

Electron cooling of the ion beam plays an important role in electron ion colliders to obtain the required high luminosity. This cooling efficiency can be enhanced by using a magnetized electron beam, where the cooling process occurs inside a solenoid field. This paper compares the predictions of ASTRA and GPT simulations to measurements made using a DC high voltage photogun producing magnetized electron beam, related to beam size and rotation angles as a function of the photogun magnetizing solenoid and other parameters.

INTRODUCTION

Electron ion colliders must provide ultra-high collision luminosity to achieve the promised physics goals. To meet this high luminosity, transverse emittance of the ion beam must be small at the electron-ion collision point. Emittance growth that results from intrabeam scattering can be controlled by electron cooling of the ion beam. The cooling efficiency can be improved by using a magnetized electron beam, where the cooling process occurs inside a solenoid field and thereby, the small helical trajectories help to increase the electron-ion interaction time while suppressing the electron-ion recombination [1, 2]. But, the radial fringe field at the entrance of the solenoid magnet creates a large additional rotational motion which adversely affects the cooling process. At the electron source, we create the electron beam inside a similar magnetic field but inducing rotational motion in the opposite direction to compensate this effect.

The generation and characterization of the magnetized electron beam was successfully conducted at Thomas Jefferson Accelerator Facility (JLab). Simultaneously, simulations were performed using ASTRA (A Space Charge Tracking Algorithm) and GPT (General Particle Tracer) programs. This paper presents details of the simulations and a comparison to beam-based measurements which help to understand the theory, both qualitatively and quantitatively and to optimize the parameters for better results.

EXPERIMENTAL SETUP

Mesaurements rely on a DC high voltage photogun operating at -300 kV. The gun has an inverted ceramic insulator, a K₂CsSb photocathode, and a green 532 nm drive DC laser with rf-structure. The transverse size of the laser

at the photocathode is set by the focusing lens of the optical transport system. The laser temporal profile is Gaussian but for these simulations, a uniform distribution was assumed with duration 25 ps.

The magnetic field at the photocathode is provided by the solenoid magnet designed to fit at the front of the gun chamber, 0.2 m away from the cathode. The magnet operates at a maximum of 400 A to provide up to 1.5 kG at photocathode.

Downstream, the beamline consists of two fluorescent YAG screen-slit combinations at 1.5 m, 2.0 m and one YAG screen at 3.75 m to measure the beam's transverse density profile at those locations, and to trace the beam rotation angles and measure the transverse emittance. Additionally, in order to focus and steer the beam four focusing solenoids and several correctors are included. A schematic diagram of the beamline is shown in Figure 1 [3].

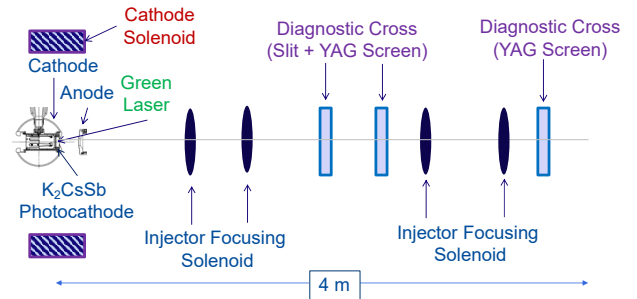


Figure 1: The diagnostic beamline.

MEASUREMENTS

For a cylindrically symmetric laminar beam with transverse rms beam sizes σ_1 at location z_1 and σ_2 at location z_2 along the beam line, the average mechanical angular momentum is given by

$$\langle L \rangle = 2 p_z \frac{\sigma_1 \sigma_2 \sin \theta}{D}, \quad (1)$$

where p_z is the longitudinal component of the electron momentum, θ is the rotation angle of the beam due to the magnetization and $D = z_2 - z_1$ [4]. Thus, in order to identify the mechanical angular momentum variation due to the magnetic field at the photocathode, transverse rms beam sizes (σ_1 , σ_2 , σ_3) at three YAG screen locations and rotation angles at the second and third YAG screen locations were measured while varying the solenoid current from 0 to 400 A. The rotation angle was obtained by inserting a slit at the location of the first YAG screen and measuring

* This work is supported by the Department of Energy, Laboratory Directed Research and Development funding, under contract DE-AC05-06OR23177

† wwije001@odu.edu

the corresponding beamlet angles at the second and third screens and by inserting a slit at second screen location and measuring the rotation angle at the third screen. For more accurate results, data tables (.SDDS file) for each case were saved and angles were calculated using a MATLAB curve fitting tool. All measurements were taken with -300 kV gun bias voltage, with the laser spot size set to 0.3 mm and displaced from the photocathode center by 0.5 mm in the vertical direction, and downstream beamline solenoids de-energized [3].

MODELLING

The beam line was modelled separately using ASTRA and GPT programs and post processing was carried out using MATLAB. The common input parameters used for the simulations are shown in Table 1.

Table 1: Input Parameters Used in Simulations

Parameter	Value
Gun voltage	-300 kV
Max magnetic field, B_z at the cathode	0.1511 T
Mean Transverse Energy	0.130 eV
Longitudinal beam size, Uniform	25 ps
Horizontal offset of the laser	0 mm
Vertical offset of the laser	0.5 mm
Number of macro particles	100000

Simulations required the electric field map of the photogun and the magnetic field map of the cathode solenoid. Electrostatic field maps were generated using POISSON for 1D, 2D and COMSOL for 3D cases. The magnetic field map was generated using Opera, and it is shown in Figure 2. It was found that the magnetic field was distorted by the steel field clamps of the focusing solenoids.

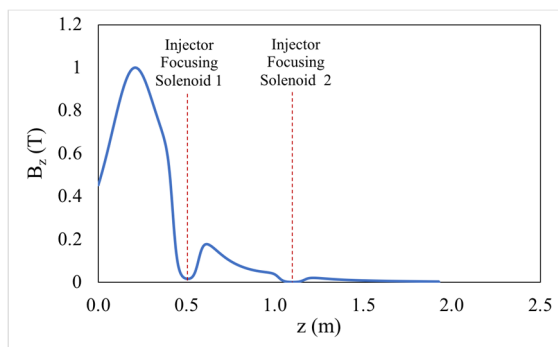


Figure 2: The magnetic field map of the cathode solenoid.

ASTRA Simulations

ASTRA was used to model the beamline with 1D electric field and 1D magnetic field map. The initial particle distribution was created using the program *generator* which comes as part of the ASTRA suite where the electron bunch emitted from the photocathode is defined in terms of number of macro particles, transverse distribu-

tions, etc., (see Table 1). In addition, a transverse beam size of 0.301 mm (Gaussian) and an initial emittance of 0.56 mm mrad/mm were used. Within the input file, three YAG screens were included as beamline elements. Additionally, in order to track off axis particle trajectories and thus to predict the pipe size for higher bunch charge simulations, few circular apertures were included along the beamline.

For rotationally symmetric fields, a table of values defining the on-axis fields, with the longitudinal position and longitudinal field of both electric (z , E_z) and magnetic (z , B_z) fields were used. Thus, radial electric and magnetic field components were deduced from the 1st to 3rd derivatives of the on-axis field [5].

In order to visualize the beam profile at each YAG screen location, beam propagation along the beam line, calculate the beam rms sizes and rotation angles at each YAG screen locations, output files were post-processed using MATLAB. Beam x_{rms} and y_{rms} sizes were calculated using the standard deviation of the x coordinates and y coordinates of each particle, respectively. Moreover, in order to calculate the rotation angle, a virtual slit was created at the 1st YAG screen and the particles are numerically tracked to the 2nd YAG screen as p_x and p_y are constants for each particle after they exit electromagnetic fields as there are no additional forces acting on them afterwards. From the gradients of the linear fits of the two YAG screen images, the rotation angle was calculated.

GPT Simulations

GPT was used to model the beamline with simulation parameters shown in Table 1 and transverse beam size 0.35 mm (Gaussian). In addition, the minimum calculation accuracy was set to 10^{-6} and three YAG screens were included as in the beamline.

The 2D electric and 1D magnetic field maps generated from POISSON and Opera were converted to General Datafile Format (GDF) before use in the GPT kernel. GPT reads the 1D table of B_z on axis and extrapolates to a cylindrical symmetric field map with 1st derivative of the on-axis field. Thus, beam transported near the z -axis gives reliable results [6].

GPT provides both time and position output where particle coordinates are output at user defined times and particle coordinates are provided at any plane in 3D space respectively [6]. GPT post processing tools GPTwin, GDF2A and GDF2A were used to visualize the beam profiles at various simulation times, extract the beam parameters (stdx, stdy, avgz) and to get Ascii output files respectively. MATLAB was used to obtain the beam profiles at each YAG screen location and to calculate the rotation angles. With GPT, in order to calculate the rotation angle, a virtual slit was created at the 1st YAG screen and particles were tracked through the data table to the 2nd YAG screen. The rotation angle was calculated from the gradient of linear fit of two screen images.

SIMULATION RESULTS ANALYSIS

Figure 3 shows the comparison between measurements, ASTRA and GPT simulations, on beam size variations and rotation angle variation as a function of cathode solenoid current.

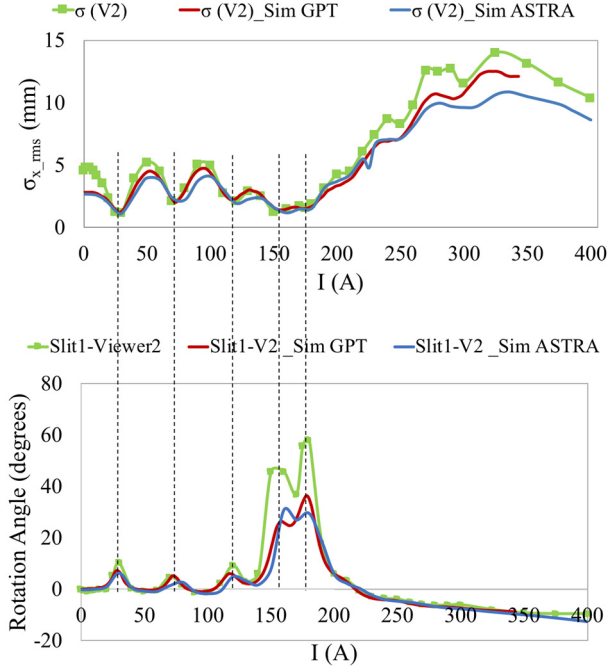


Figure 3: Beam rms size variation with the cathode solenoid current (top), rotation angle variation versus cathode solenoid current (bottom) for slit 1-YAG screen 2 combination. Color code: green measured values, red GPT, and blue ASTRA.

The plots show good agreement between measurements and simulations. The top plot shows oscillations in the beam size, converging and diverging with the solenoid current, a behavior known as mismatch oscillations [7]. This occurs due to the non-uniform magnetic field of the gun solenoid magnet shown in Figure 2. The magnetic force from the cathode solenoid does not match the initial emittance force. These imbalanced forces result in repeated focusing of the beam within the gun solenoid.

The bottom plot shows the rotation angle variation with the solenoid current, showing an opposite pattern to the top plot, which is reasonable. When beam size decreases, which means the beam is converging and the rotation angle should increase and vice-versa. But some cathode solenoid currents result in unexpected negative angles (large angles). This occurs when a converging beam at the slit is being examined by the viewer downstream of the focal point of the converging beam. According to this concept a general form for the rotation angle θ_{rot} in equation (1) was formulated as follows

$$\theta_{rot} = \tan^{-1} \frac{\dot{\theta} D/v_z}{1-D/f}, \quad (2)$$

where $\dot{\theta}$ indicates the rotation due to the magnetization, v_z is the velocity in z direction and f is the focal length due to the convergence. Thus, when focusing is achieved before the viewer ($D > f$), the denominator is negative, and it is possible for the observed rotation angle to be in the second quadrant. When beam is diverging ($f < 0$) or beam at the slit is at a waist, the observed rotation angle should be in first quadrant.

The measured beam size values at YAG screens are significantly higher than the simulated values, for low current settings of the gun magnetizing solenoid, suggesting our electric field map is inaccurate. A 3D electric field map could provide better agreement. In addition, accuracy of the measured laser spot size at the photocathode and horizontal and vertical beam offsets may also cause small disagreements.

CONCLUSION

In summary the magnetized beam generated at JLab is successfully modelled using ASTRA and GPT software and showing reasonably good agreement with the measurements. More accurate field maps and input parameters may lead to even better agreement with the measurements. Simulations have helped to understand the physics of mismatch oscillations and rotation angles with large angles. Nonetheless a general formula is presented to calculate the rotation angle for both converging and diverging beams.

ACKNOWLEDGMENTS

This work is supported by the Department of Energy, under contract DE-AC05-06OR23177 and the Laboratory Directed Research and Development program.

REFERENCES

- [1] Ya. Derbenev and A. Skrinsky, "Magnetization effect in Electron Cooling," *Fiz. Plazmy*, vol. 4, 492, 1978; [*Sov. J. Plasma Phys.* 4, 273 (1978)].
- [2] R. Brinkmann, Y. Derbenev and K. Flöttmann, "A Low Emittance Flat-beam Electron Source for Linear Colliders," *Phys. Rev. ST Accel. Beams*, vol. 4, p. 053501, 2001.
- [3] M.A. Mamun *et al.*, "Production of Magnetized Electron Beam from a DC High Voltage Photogun," presented at the 9th Int. Particle Accelerator Conf. (IPAC'18), Vancouver, Canada, Apr.-May 2018, paper THPMK108.
- [4] Y.E. Sun, P. Piot, K.J. Kim, N. Barov, S. Lidia, J. Santucci, R. Tikhoplav, and J. Wennerberg, "Generation of Angular Momentum Dominated Electron Beams from a Photoinjector", *Phys. Rev. ST Accel. Beams*, vol. 7, p. 123501, Dec. 2004.
- [5] K. Flöttmann, "ASTRA : A Space charge Tracking Algorithm", online user manual http://www.desy.de/~mpyf10/Astra_dokumentation
- [6] S.B. van der Geer and M.J. de Loos, "General Particle Tracer" user manual.
- [7] M. Reiser, *Theory and Design of Charged Particle Beams*, New York, NY, USA: Wiley, 1995